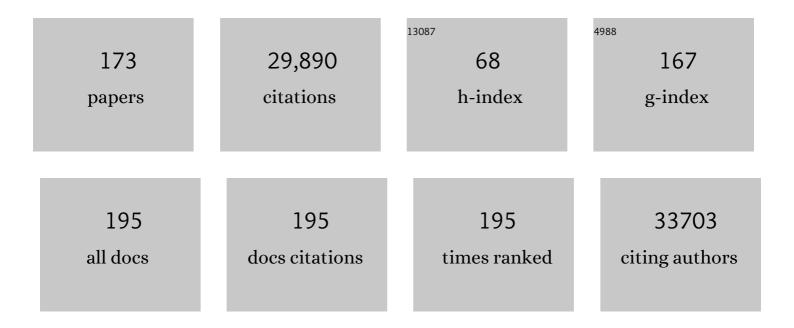
List of Publications by Year in descending order

Source: https://exaly.com/author-pdf/2778005/publications.pdf Version: 2024-02-01



#	Article	IF	CITATIONS
1	Single-Layer MoS ₂ Phototransistors. ACS Nano, 2012, 6, 74-80.	7.3	3,103
2	Grapheneâ€Based Materials: Synthesis, Characterization, Properties, and Applications. Small, 2011, 7, 1876-1902.	5.2	2,239
3	Singleâ€Layer Semiconducting Nanosheets: Highâ€Yield Preparation and Device Fabrication. Angewandte Chemie - International Edition, 2011, 50, 11093-11097.	7.2	1,517
4	Preparation and Applications of Mechanically Exfoliated Single-Layer and Multilayer MoS ₂ and WSe ₂ Nanosheets. Accounts of Chemical Research, 2014, 47, 1067-1075.	7.6	1,374
5	Fabrication of Single―and Multilayer MoS ₂ Filmâ€Based Fieldâ€Effect Transistors for Sensing NO at Room Temperature. Small, 2012, 8, 63-67.	5.2	1,346
6	Synthesis of Few‣ayer MoS ₂ Nanosheetâ€Coated TiO ₂ Nanobelt Heterostructures for Enhanced Photocatalytic Activities. Small, 2013, 9, 140-147.	5.2	1,166
7	Fabrication of Flexible MoS ₂ Thinâ€Film Transistor Arrays for Practical Gas‧ensing Applications. Small, 2012, 8, 2994-2999.	5.2	817
8	Three-dimensional graphene materials: preparation, structures and application in supercapacitors. Energy and Environmental Science, 2014, 7, 1850-1865.	15.6	773
9	Graphene-based electronic sensors. Chemical Science, 2012, 3, 1764.	3.7	663
10	Graphene and Grapheneâ€Based Materials for Energy Storage Applications. Small, 2014, 10, 3480-3498.	5.2	653
11	Electrochemical Deposition of ZnO Nanorods on Transparent Reduced Graphene Oxide Electrodes for Hybrid Solar Cells. Small, 2010, 6, 307-312.	5.2	626
12	Surface strategies for catalytic CO ₂ reduction: from two-dimensional materials to nanoclusters to single atoms. Chemical Society Reviews, 2019, 48, 5310-5349.	18.7	607
13	Carbon Fiber Aerogel Made from Raw Cotton: A Novel, Efficient and Recyclable Sorbent for Oils and Organic Solvents. Advanced Materials, 2013, 25, 5916-5921.	11.1	600
14	25th Anniversary Article: Hybrid Nanostructures Based on Twoâ€Dimensional Nanomaterials. Advanced Materials, 2014, 26, 2185-2204.	11.1	579
15	Centimeter-Long and Large-Scale Micropatterns of Reduced Graphene Oxide Films: Fabrication and Sensing Applications. ACS Nano, 2010, 4, 3201-3208.	7.3	571
16	Organic Photovoltaic Devices Using Highly Flexible Reduced Graphene Oxide Films as Transparent Electrodes. ACS Nano, 2010, 4, 5263-5268.	7.3	566
17	Mechanical Exfoliation and Characterization of Single―and Few‣ayer Nanosheets of WSe ₂ , TaS ₂ , and TaSe ₂ . Small, 2013, 9, 1974-1981.	5.2	544
18	An Effective Method for the Fabrication of Few‣ayerâ€Thick Inorganic Nanosheets. Angewandte Chemie - International Edition, 2012, 51, 9052-9056.	7.2	520

#	Article	lF	CITATIONS
19	Hierarchical hollow spheres composed of ultrathin Fe2O3 nanosheets for lithium storage and photocatalytic water oxidation. Energy and Environmental Science, 2013, 6, 987.	15.6	404
20	Grapheneâ€Based Materials for Solar Cell Applications. Advanced Energy Materials, 2014, 4, 1300574.	10.2	398
21	Electrochemically Reduced Single‣ayer MoS ₂ Nanosheets: Characterization, Properties, and Sensing Applications. Small, 2012, 8, 2264-2270.	5.2	373
22	A general method for the large-scale synthesis of uniform ultrathin metal sulphide nanocrystals. Nature Communications, 2012, 3, 1177.	5.8	368
23	MoS2 nanoflower-decorated reduced graphene oxide paper for high-performance hydrogen evolution reaction. Nanoscale, 2014, 6, 5624.	2.8	320
24	Transparent, Flexible, All-Reduced Graphene Oxide Thin Film Transistors. ACS Nano, 2011, 5, 5038-5044.	7.3	305
25	Optical Identification of Single―and Few‣ayer MoS ₂ Sheets. Small, 2012, 8, 682-686.	5.2	290
26	Au Nanoparticleâ€Modified MoS ₂ Nanosheetâ€Based Photoelectrochemical Cells for Water Splitting. Small, 2014, 10, 3537-3543.	5.2	265
27	MnO ₂ â€Based Materials for Environmental Applications. Advanced Materials, 2021, 33, e2004862.	11.1	252
28	Surface enhanced Raman scattering of Ag or Au nanoparticle-decorated reduced graphene oxide for detection of aromatic molecules. Chemical Science, 2011, 2, 1817.	3.7	249
29	A general salt-resistant hydrophilic/hydrophobic nanoporous double layer design for efficient and stable solar water evaporation distillation. Materials Horizons, 2018, 5, 1143-1150.	6.4	232
30	Layer Thinning and Etching of Mechanically Exfoliated MoS ₂ Nanosheets by Thermal Annealing in Air. Small, 2013, 9, 3314-3319.	5.2	229
31	Bulk Heterojunction Polymer Memory Devices with Reduced Graphene Oxide as Electrodes. ACS Nano, 2010, 4, 3987-3992.	7.3	215
32	Rare-earth-containing perovskite nanomaterials: design, synthesis, properties and applications. Chemical Society Reviews, 2020, 49, 1109-1143.	18.7	211
33	Fabrication of Flexible, Allâ€Reduced Graphene Oxide Nonâ€Volatile Memory Devices. Advanced Materials, 2013, 25, 233-238.	11.1	207
34	Allâ€Carbon Electronic Devices Fabricated by Directly Grown Singleâ€Walled Carbon Nanotubes on Reduced Graphene Oxide Electrodes. Advanced Materials, 2010, 22, 3058-3061.	11.1	201
35	Carbon Microbelt Aerogel Prepared by Waste Paper: An Efficient and Recyclable Sorbent for Oils and Organic Solvents. Small, 2014, 10, 3544-3550.	5.2	196
36	A Universal, Rapid Method for Clean Transfer of Nanostructures onto Various Substrates. ACS Nano, 2014, 8, 6563-6570.	7.3	192

#	Article	IF	CITATIONS
37	Periodic stacking of 2D charged sheets: Self-assembled superlattice of Ni–Al layered double hydroxide (LDH) and reduced graphene oxide. Nano Energy, 2016, 20, 185-193.	8.2	188
38	Real-time DNA detection using Pt nanoparticle-decorated reduced graphene oxide field-effect transistors. Nanoscale, 2012, 4, 293-297.	2.8	185
39	Fabrication of Graphene Nanomesh by Using an Anodic Aluminum Oxide Membrane as a Template. Advanced Materials, 2012, 24, 4138-4142.	11.1	183
40	A facile, relative green, and inexpensive synthetic approach toward large-scale production of SnS2 nanoplates for high-performance lithium-ion batteries. Nanoscale, 2013, 5, 1456.	2.8	177
41	Anion-redox nanolithia cathodes for Li-ion batteries. Nature Energy, 2016, 1, .	19.8	171
42	Electrochemical Deposition of Semiconductor Oxides on Reduced Graphene Oxide-Based Flexible, Transparent, and Conductive Electrodes. Journal of Physical Chemistry C, 2010, 114, 11816-11821.	1.5	159
43	Noble-Metal-Free Multicomponent Nanointegration for Sustainable Energy Conversion. Chemical Reviews, 2021, 121, 10271-10366.	23.0	156
44	Znln ₂ S ₄ â€Based Photocatalysts for Energy and Environmental Applications. Small Methods, 2021, 5, e2100887.	4.6	153
45	Heterogeneous bimetallic sulfides based seawater electrolysis towards stable industrial-level large current density. Applied Catalysis B: Environmental, 2021, 291, 120071.	10.8	150
46	Memory Devices Using a Mixture of MoS ₂ and Graphene Oxide as the Active Layer. Small, 2013, 9, 727-731.	5.2	144
47	Regulating the active species of Ni(OH) ₂ using CeO ₂ : 3D CeO ₂ /Ni(OH) ₂ /carbon foam as an efficient electrode for the oxygen evolution reaction. Chemical Science, 2017, 8, 3211-3217.	3.7	141
48	Coupling and Stacking Order of ReS ₂ Atomic Layers Revealed by Ultralow-Frequency Raman Spectroscopy. Nano Letters, 2016, 16, 1404-1409.	4.5	139
49	Enhancement of Photogenerated Electron Transport in Dyeâ€Sensitized Solar Cells with Introduction of a Reduced Graphene Oxide–TiO ₂ Junction. Chemistry - A European Journal, 2011, 17, 10832-10837.	1.7	133
50	Preparation of MoS ₂ –MoO ₃ Hybrid Nanomaterials for Lightâ€Emitting Diodes. Angewandte Chemie - International Edition, 2014, 53, 12560-12565.	7.2	133
51	Synthesis of Fe3O4 and Pt nanoparticles on reduced graphene oxide and their use as a recyclable catalyst. Nanoscale, 2012, 4, 2478.	2.8	131
52	Full Solutionâ€Processed Synthesis of All Metal Oxideâ€Based Treeâ€like Heterostructures on Fluorineâ€Doped Tin Oxide for Water Splitting. Advanced Materials, 2012, 24, 5374-5378.	11.1	131
53	Postchemistry of Organic Particles: When TTF Microparticles Meet TCNQ Microstructures in Aqueous Solution. Journal of the American Chemical Society, 2010, 132, 6926-6928.	6.6	125
54	Colloidal synthesis of 1T' phase dominated WS2 towards endurable electrocatalysis. Nano Energy, 2018, 50, 176-181.	8.2	123

#	Article	IF	CITATIONS
55	Atomically Dispersed Indium Sites for Selective CO ₂ Electroreduction to Formic Acid. ACS Nano, 2021, 15, 5671-5678.	7.3	121
56	Crystal Structure and Phototransistor Behavior of N-Substituted Heptacence. ACS Applied Materials & Interfaces, 2012, 4, 1883-1886.	4.0	118
57	Preparation, characterization, and photoswitching/light-emitting behaviors of coronene nanowires. Journal of Materials Chemistry, 2011, 21, 1423-1427.	6.7	116
58	Oxygen vacancies activating surface reactivity to favor charge separation and transfer in nanoporous BiVO4 photoanodes. Applied Catalysis B: Environmental, 2021, 281, 119477.	10.8	116
59	Multilayer Stacked Lowâ€Temperatureâ€Reduced Graphene Oxide Films: Preparation, Characterization, and Application in Polymer Memory Devices. Small, 2010, 6, 1536-1542.	5.2	113
60	Aminosilane Micropatterns on Hydroxyl-Terminated Substrates: Fabrication and Applications. Langmuir, 2010, 26, 5603-5609.	1.6	98
61	Synthesis, Characterization, and Physical Properties of a Conjugated Heteroacene: 2â€Methylâ€1,4,6,7,8,9â€hexaphenylbenz(<i>g</i>)isoquinolinâ€3(2 <i>H</i>)â€one (BIQ). Chemistry - an Asian Journal, 2011, 6, 856-862.	1.7	95
62	Chemical Reaction Between Ag Nanoparticles and TCNQ Microparticles in Aqueous Solution. Small, 2011, 7, 1242-1246.	5.2	92
63	Electrochemical deposition of Cl-doped n-type Cu ₂ 0 on reduced graphene oxide electrodes. Journal of Materials Chemistry, 2011, 21, 3467-3470.	6.7	91
64	Rareâ€Earth Incorporated Alloy Catalysts: Synthesis, Properties, and Applications. Advanced Materials, 2021, 33, e2005988.	11.1	84
65	Photoanode Current of Large–Area MoS ₂ Ultrathin Nanosheets with Vertically Mesh–Shaped Structure on Indium Tin Oxide. ACS Applied Materials & Interfaces, 2014, 6, 5983-5987.	4.0	79
66	Low-Temperature in Situ Growth of Graphene on Metallic Substrates and Its Application in Anticorrosion. ACS Applied Materials & amp; Interfaces, 2016, 8, 502-510.	4.0	78
67	Fabrication of nanoelectrode ensembles by electrodepositon of Au nanoparticles on single-layer graphene oxide sheets. Nanoscale, 2012, 4, 2728.	2.8	76
68	Nanolithography of Single-Layer Graphene Oxide Films by Atomic Force Microscopy. Langmuir, 2010, 26, 6164-6166.	1.6	68
69	Emerging Strategies for CO ₂ Photoreduction to CH ₄ : From Experimental to Dataâ€Driven Design. Advanced Energy Materials, 2022, 12, .	10.2	68
70	Oriented Molecular Attachments Through Sol–Gel Chemistry for Synthesis of Ultrathin Hydrated Vanadium Pentoxide Nanosheets and Their Applications. Small, 2013, 9, 716-721.	5.2	67
71	Lanthanide doping induced electrochemical enhancement of Na ₂ Ti ₃ O ₇ anodes for sodium-ion batteries. Chemical Science, 2018, 9, 3421-3425.	3.7	66
72	Room temperature stable CO _{<i>x</i>} -free H ₂ production from methanol with magnesium oxide nanophotocatalysts. Science Advances, 2016, 2, e1501425.	4.7	62

#	Article	IF	CITATIONS
73	High‥ield Electrochemical Production of Largeâ€Sized and Thinly Layered NiPS ₃ Flakes for Overall Water Splitting. Small, 2019, 15, e1902427.	5.2	62
74	Solid Nanoporosity Governs Catalytic CO ₂ and N ₂ Reduction. ACS Nano, 2020, 14, 7734-7759.	7.3	59
75	2D Materials Based on Main Group Element Compounds: Phases, Synthesis, Characterization, and Applications. Advanced Functional Materials, 2020, 30, 2001127.	7.8	58
76	General Bottom-Up Colloidal Synthesis of Nano-Monolayer Transition-Metal Dichalcogenides with High 1T′-Phase Purity. Journal of the American Chemical Society, 2022, 144, 4863-4873.	6.6	58
77	2D materials inks toward smart flexible electronics. Materials Today, 2021, 50, 116-148.	8.3	57
78	Mechanisms and Applications of Steady-State Photoluminescence Spectroscopy in Two-Dimensional Transition-Metal Dichalcogenides. ACS Nano, 2020, 14, 14579-14604.	7.3	56
79	Structuralâ€Phase Catalytic Redox Reactions in Energy and Environmental Applications. Advanced Materials, 2020, 32, e1905739.	11.1	56
80	Bottomâ€Up Preparation of Porous Metalâ€Oxide Ultrathin Sheets with Adjustable Composition/Phases and Their Applications. Small, 2011, 7, 3458-3464.	5.2	55
81	A review of energy bandgap engineering in Ill–V semiconductor alloys for mid-infrared laser applications. Solid-State Electronics, 2007, 51, 6-15.	0.8	53
82	Dataâ€Driven Materials Innovation and Applications. Advanced Materials, 2022, 34, e2104113.	11.1	51
83	Nucleation Mechanism of Electrochemical Deposition of Cu on Reduced Graphene Oxide Electrodes. Journal of Physical Chemistry C, 2011, 115, 15973-15979.	1.5	50
84	Spontaneous Formation of Noble―and Heavyâ€Metalâ€Free Alloyed Semiconductor Quantum Rods for Efficient Photocatalysis. Advanced Materials, 2018, 30, e1803351.	11.1	47
85	Preparation, characterization, physical properties, and photoconducting behaviour of anthracene derivative nanowires. Nanoscale, 2011, 3, 4720.	2.8	46
86	Sustainable Nanoplasmonâ€Enhanced Photoredox Reactions: Synthesis, Characterization, and Applications. Advanced Energy Materials, 2020, 10, 2002402.	10.2	44
87	InVO4-based photocatalysts for energy and environmental applications. Chemical Engineering Journal, 2022, 428, 131145.	6.6	44
88	Advancement of Bismuthâ€Based Materials for Electrocatalytic and Photo(electro)catalytic Ammonia Synthesis. Advanced Functional Materials, 2022, 32, 2106713.	7.8	44
89	Enhanced transport in transistor by tuning transition-metal oxide electronic states interfaced with diamond. Science Advances, 2018, 4, eaau0480.	4.7	42
90	Bandgap engineered g-C3N4 and its graphene composites for stable photoreduction of CO2 to methanol. Carbon, 2022, 192, 101-108.	5.4	42

#	Article	IF	CITATIONS
91	Solution-Processed Nanocrystalline TiO ₂ Buffer Layer Used for Improving the Performance of Organic Photovoltaics. ACS Applied Materials & Interfaces, 2011, 3, 1063-1067.	4.0	40
92	Colloidal Single‣ayer Photocatalysts for Methanolâ€Storable Solar H ₂ Fuel. Advanced Materials, 2019, 31, e1905540.	11.1	39
93	Nonepitaxial Goldâ€Tipped ZnSe Hybrid Nanorods for Efficient Photocatalytic Hydrogen Production. Small, 2020, 16, e1902231.	5.2	37
94	Assembly of Graphene Oxide and Au0.7Ag0.3 Alloy Nanoparticles on SiO2: A New Raman Substrate with Ultrahigh Signal-to-Background Ratio. Journal of Physical Chemistry C, 2011, 115, 24080-24084.	1.5	36
95	A carbon monoxide gas sensor using oxygen plasma modified carbon nanotubes. Nanotechnology, 2012, 23, 425502.	1.3	35
96	High-Temperature Thermoelectric Monolayer Bi ₂ TeSe ₂ with High Power Factor and Ultralow Thermal Conductivity. ACS Applied Energy Materials, 2022, 5, 2564-2572.	2.5	35
97	Quantifying Quasiâ€Fermi Level Splitting and Mapping its Heterogeneity in Atomically Thin Transition Metal Dichalcogenides. Advanced Materials, 2019, 31, e1900522.	11.1	34
98	Periodic nanostructures: preparation, properties and applications. Chemical Society Reviews, 2021, 50, 6423-6482.	18.7	34
99	Boosting Thermoelectric Performance of 2D Transition-Metal Dichalcogenides by Complex Cluster Substitution: The Role of Octahedral Au ₆ Clusters. ACS Applied Energy Materials, 2021, 4, 12163-12176.	2.5	33
100	Waterproof molecular monolayers stabilize 2D materials. Proceedings of the National Academy of Sciences of the United States of America, 2019, 116, 20844-20849.	3.3	32
101	Machine learning accelerated calculation and design of electrocatalysts for CO ₂ reduction. SmartMat, 2022, 3, 68-83.	6.4	31
102	MOF-on-MOF nanoarchitecturing of Fe2O3@ZnFe2O4 radial-heterospindles towards multifaceted superiorities for acetone detection. Chemical Engineering Journal, 2022, 442, 136094.	6.6	31
103	Photoactivity and Stability Coâ€Enhancement: When Localized Plasmons Meet Oxygen Vacancies in MgO. Small, 2018, 14, e1803233.	5.2	28
104	A Diamond:H/WO ₃ Metal–Oxide–Semiconductor Field-Effect Transistor. IEEE Electron Device Letters, 2018, 39, 540-543.	2.2	27
105	Synergizing Phase and Cavity in CoMoO <i>_x</i> S <i>_y</i> Yolk–Shell Anodes to Coâ€Enhance Capacity and Rate Capability in Sodium Storage. Small, 2020, 16, e2002487.	5.2	27
106	The data-intensive scientific revolution occurring where two-dimensional materials meet machine learning. Cell Reports Physical Science, 2021, 2, 100482.	2.8	26
107	Rare earth element based single-atom catalysts: synthesis, characterization and applications in photo/electro-catalytic reactions. Nanoscale Horizons, 2021, 7, 31-40.	4.1	26
108	Mesoporous ZnAl2Si10O24 nanofertilizers enable high yield of Oryza sativa L Scientific Reports, 2020, 10, 10841.	1.6	25

#	Article	IF	CITATIONS
109	Machine Learningâ€Aided Crystal Facet Rational Design with Ionic Liquid Controllable Synthesis. Small, 2021, 17, e2100024.	5.2	24
110	Growth of dandelion-shaped CuInSe ₂ nanostructures by a two-step solvothermal process. Nanotechnology, 2011, 22, 195607.	1.3	23
111	Gold Nanotip Array for Ultrasensitive Electrochemical Sensing and Spectroscopic Monitoring. Small, 2013, 9, 2260-2265.	5.2	23
112	Low temperature growth of graphene on Cu–Ni alloy nanofibers for stable, flexible electrodes. Nanoscale, 2014, 6, 5110.	2.8	23
113	Emission Control from Transition Metal Dichalcogenide Monolayers by Aggregation-Induced Molecular Rotors. ACS Nano, 2020, 14, 7444-7453.	7.3	23
114	Twist-driven wide freedom of indirect interlayer exciton emission in MoS2/WS2 heterobilayers. Cell Reports Physical Science, 2021, 2, 100509.	2.8	23
115	Nano Polymorphismâ€Enabled Redox Electrodes for Rechargeable Batteries. Advanced Materials, 2021, 33, e2004920.	11.1	23
116	Rational Synthesis of Triangular Au–Ag ₂ S Hybrid Nanoframes with Effective Photoresponses. Chemistry - A European Journal, 2014, 20, 2742-2745.	1.7	22
117	Phosphineâ€Free, Lowâ€Temperature Synthesis of Tetrapodâ€Shaped CdS and Its Hybrid with Au Nanoparticles. Small, 2014, 10, 4727-4734.	5.2	20
118	Periodic AuAgâ€Ag ₂ S Heterostructured Nanowires. Small, 2014, 10, 479-482.	5.2	20
119	Emerging Synthesis Strategies of 2D MOFs for Electrical Devices and Integrated Circuits. Small, 2022, 18, .	5.2	19
120	A new method of two-step growth of InAs/GaAs quantum dots with higher density and more size uniformity. Nanotechnology, 2006, 17, 295-299.	1.3	17
121	Thickness-tunable growth of ultra-large, continuous and high-dielectric h-BN thin films. Journal of Materials Chemistry C, 2019, 7, 1871-1879.	2.7	17
122	Electrocatalysis enabled transformation of earth-abundant water, nitrogen and carbon dioxide for a sustainable future. Materials Advances, 2022, 3, 1359-1400.	2.6	17
123	TaS2 nanosheet-based room-temperature dosage meter for nitric oxide. APL Materials, 2014, 2, .	2.2	16
124	A thermally insulated solar evaporator coupled with a passive condenser for freshwater collection. Journal of Materials Chemistry A, 2021, 9, 22428-22439.	5.2	16
125	An Experimentally Verified LCâ€MS Protocol toward an Economical, Reliable, and Quantitative Isotopic Analysis in Nitrogen Reduction Reactions. Small Methods, 2021, 5, e2000694.	4.6	16
126	Effects of InxGa1â^'xAs matrix layer on InAs quantum dot formation and their emission wavelength. Journal of Applied Physics, 2006, 100, 033109.	1.1	15

#	Article	IF	CITATIONS
127	Organic–Rare Earth Hybrid Anode with Superior Cyclability for Lithium Ion Battery. Advanced Materials Interfaces, 2020, 7, 1902168.	1.9	15
128	Effect of rapid thermal annealing on the ordering of AlInP grown by metal-organic vapor-phase epitaxy. Applied Physics Letters, 2005, 87, 181906.	1.5	14
129	Plasmonically enhanced photoluminescence of monolayer MoS ₂ via nanosphere lithography-templated gold metasurfaces. Nanophotonics, 2021, 10, 1733-1740.	2.9	14
130	Generation of Dual Patterns of Metal Oxide Nanomaterials Based on Seed-Mediated Selective Growth. Langmuir, 2010, 26, 4616-4619.	1.6	12
131	Controlled CVD growth of Cu–Sb alloy nanostructures. Nanotechnology, 2011, 22, 325602.	1.3	12
132	Colloidal quasi-one-dimensional dual semiconductor core/shell nanorod couple heterostructures with blue fluorescence. Nanoscale, 2019, 11, 10190-10197.	2.8	12
133	All room-temperature synthesis, N2 photofixation and reactivation over 2D cobalt oxides. Applied Catalysis B: Environmental, 2022, 304, 121001.	10.8	11
134	Effects of growth conditions on InAs quantum dot formation by metal-organic chemical vapor deposition using tertiarybutylarsine in pure N2 ambient. Journal of Applied Physics, 2006, 99, 124306.	1.1	10
135	Photo/electrochemical Carbon Dioxide Conversion into C ₃₊ Hydrocarbons: Reactivity and Selectivity. ChemNanoMat, 2021, 7, 969-981.	1.5	10
136	Selective N2/H2O adsorption onto 2D amphiphilic amorphous photocatalysts for ambient gas-phase nitrogen fixation. Applied Catalysis B: Environmental, 2021, 294, 120240.	10.8	10
137	Rod-coating all-solution fabrication of double functional graphene oxide films for flexible alternating current (AC)-driven light-emitting diodes. RSC Advances, 2014, 4, 55671-55676.	1.7	8
138	Mid-infrared emissive InAsSb quantum dots grown by metal–organic chemical vapor deposition. CrystEngComm, 2013, 15, 604-608.	1.3	7
139	Simulation-guided nanofabrication of high-quality practical tungsten probes. RSC Advances, 2020, 10, 24280-24287.	1.7	7
140	Integration of data-intensive, machine learning and robotic experimental approaches for accelerated discovery of catalysts in renewable energy-related reactions. Materials Reports Energy, 2021, 1, 100049.	1.7	7
141	Thermal annealing effect on GaNAs epilayers with different nitrogen compositions grown by MOCVD. Journal of Crystal Growth, 2007, 307, 229-234.	0.7	6
142	Formation of mid-infrared emissive InAs quantum dots on a graded InxGa1â^'xAs/InP matrix with a more uniform size and higher density under safer growth conditions. Nanotechnology, 2006, 17, 1646-1650.	1.3	5
143	Argon-plasma-induced InAs/InGaAs/InP quantum dot intermixing. Nanotechnology, 2006, 17, 4664-4667.	1.3	5
144	Zero-emission multivalorization of light alcohols with self-separable pure H2 fuel. Applied Catalysis B: Environmental, 2021, 292, 120212.	10.8	5

#	Article	IF	CITATIONS
145	Thermal Transport and Mechanical Properties of Layered Oxychalcogenides LaCuOX (X = S, Se, and Te). ACS Applied Energy Materials, 2022, 5, 6943-6951.	2.5	5
146	Layered Nanomaterials: Fabrication of Single- and Multilayer MoS2 Film-Based Field-Effect Transistors for Sensing NO at Room Temperature (Small 1/2012). Small, 2012, 8, 2-2.	5.2	4
147	NIR-plasmon-enhanced Systems for Energy Conversion and Environmental Remediation. Chemical Research in Chinese Universities, 2020, 36, 1000-1005.	1.3	4
148	Mid-Infrared Emission From InAs Quantum Dots Grown by Metal–Organic Vapor Phase Epitaxy. IEEE Nanotechnology Magazine, 2006, 5, 683-686.	1.1	3
149	Selective Intermixing of InAs/InGaAs/InP Quantum Dot Structure With Large Energy Band Gap Tuning. IEEE Nanotechnology Magazine, 2008, 7, 422-426.	1.1	3
150	Polarization insensitive gain medium with hybrid strained quantum well. Optics and Laser Technology, 2002, 34, 595-597.	2.2	2
151	Study of InAs/GaAs quantum dots grown by MOVPE under the safer growth conditions. Journal of Nanoparticle Research, 2007, 9, 877-884.	0.8	2
152	MOVPE growth of AlxIn1â^'xP using tertiarybutylphosphine in pure N2 ambient. Thin Solid Films, 2007, 515, 4454-4458.	0.8	2
153	Water Splitting: Au Nanoparticle-Modified MoS2Nanosheet-Based Photoelectrochemical Cells for Water Splitting (Small 17/2014). Small, 2014, 10, 3536-3536.	5.2	2
154	Solar Cells: Quantifying Quasiâ€Fermi Level Splitting and Mapping its Heterogeneity in Atomically Thin Transition Metal Dichalcogenides (Adv. Mater. 25/2019). Advanced Materials, 2019, 31, 1970180.	11.1	2
155	InAs self-assembled quantum dots on GaAs/InP by low-pressure metal-organic chemical vapour deposition. Semiconductor Science and Technology, 2001, 16, 715-719.	1.0	1
156	Below bandgap emission with intensity higher than bandâ€ŧoâ€band transition in GaAsN. Physica Status Solidi C: Current Topics in Solid State Physics, 2008, 5, 464-466.	0.8	1
157	First-step nucleation growth dependence of InAs/InGaAs/InP quantum dot formation in two-step growth. Nanotechnology, 2008, 19, 085603.	1.3	1
158	Photoluminescence of InAs quantum dots embedded in graded InGaAs barriers. Journal of Nanoparticle Research, 2009, 11, 1947-1955.	0.8	1
159	CdS: Phosphineâ€Free, Lowâ€Temperature Synthesis of Tetrapodâ€5haped CdS and Its Hybrid with Au Nanoparticles (Small 22/2014). Small, 2014, 10, 4726-4726.	5.2	1
160	Lithiumâ€lon Batteries: Organic–Rare Earth Hybrid Anode with Superior Cyclability for Lithium Ion Battery (Adv. Mater. Interfaces 9/2020). Advanced Materials Interfaces, 2020, 7, 2070051.	1.9	1
161	One-Step Carbothermal Synthesis of Super Nanoadsorbents for Rapid and Recyclable Wastewater Treatment. Crystals, 2021, 11, 75.	1.0	1
162	InP Based Quantum Dots for Long Wavelength Emissions and Their Post-Growth Bandgap Tuning. Journal of Nanoelectronics and Optoelectronics, 2015, 10, 151-156.	0.1	1

ZONGYOU YIN

#	Article	IF	CITATIONS
163	Stable two-dimensional lead iodide hybrid materials for light detection and broadband photoluminescence. Materials Chemistry Frontiers, 2021, 6, 71-77.	3.2	1
164	Data-driven engineering descriptor and refined scale relations for predicting bubble departure diameter. International Journal of Heat and Mass Transfer, 2022, 195, 123078.	2.5	1
165	Characteristic study of InAs self-assembled quantum dots on GaAs/InP. , 2001, , .		0
166	Characteristics of ZnO film grown by MOCVD. , 2001, , .		0
167	Studying the mechanism of ordered growth of InAs quantum dots on GaAs/InP. Optics and Laser Technology, 2001, 33, 507-509.	2.2	0
168	Ordering InAs Quantum Dots Formation on GaAs/InP by Low Pressure Metal-Organic Chemical Vapor Deposition. Japanese Journal of Applied Physics, 2001, 40, 5889-5892.	0.8	0
169	MOVPE growth of InAs quantum dots for mid-IR applications. Transactions of Nonferrous Metals Society of China, 2006, 16, s25-s28.	1.7	0
170	MOVPE GROWTH OF THE InP BASED MID-IR EMISSION QUANTUM DOT STRUCTURES. Journal of Molecular and Engineering Materials, 2013, 01, 1350002.	0.9	0
171	Photocatalysis: Spontaneous Formation of Noble- and Heavy-Metal-Free Alloyed Semiconductor Quantum Rods for Efficient Photocatalysis (Adv. Mater. 39/2018). Advanced Materials, 2018, 30, 1870296.	11.1	0
172	Photocatalysts: Colloidal Single‣ayer Photocatalysts for Methanol‣torable Solar H ₂ Fuel (Adv. Mater. 49/2019). Advanced Materials, 2019, 31, 1970348.	11.1	0
173	Photocatalytic Hydrogen Production: Nonepitaxial Goldâ€Tipped ZnSe Hybrid Nanorods for Efficient Photocatalytic Hydrogen Production (Small 12/2020). Small, 2020, 16, 2070066.	5.2	Ο